

Secondary electron deposition mechanism of carbon contamination

Adam F. G. Leontowich and Adam P. Hitchcock

Citation: *J. Vac. Sci. Technol. B* **30**, 030601 (2012); doi: 10.1116/1.3698602

View online: <http://dx.doi.org/10.1116/1.3698602>

View Table of Contents: <http://avspublications.org/resource/1/JVTBD9/v30/i3>

Published by the AVS: Science & Technology of Materials, Interfaces, and Processing

Related Articles

Secondary electron yield on cryogenic surfaces as a function of physisorbed gases

J. Vac. Sci. Technol. A **30**, 051401 (2012)

Modeling of charging effect on ion induced secondary electron emission from nanostructured materials

J. Vac. Sci. Technol. B **29**, 06F901 (2011)

Methods for measurement of electron emission yield under low energy electron-irradiation by collector method and Kelvin probe method

J. Vac. Sci. Technol. A **28**, 1122 (2010)

Synthesis and electron emission properties of MgO nanowires

J. Vac. Sci. Technol. B **28**, C2B20 (2010)

Roles of secondary electrons and sputtered atoms in ion-beam-induced deposition

J. Vac. Sci. Technol. B **27**, 2718 (2009)

Additional information on *J. Vac. Sci. Technol. B*

Journal Homepage: <http://avspublications.org/jvstb>

Journal Information: http://avspublications.org/jvstb/about/about_the_journal

Top downloads: http://avspublications.org/jvstb/top_20_most_downloaded

Information for Authors: http://avspublications.org/jvstb/authors/information_for_contributors

ADVERTISEMENT

AVS 59th International Symposium & Exhibition
October 28 - November 2, 2012 • Tampa, Florida

AVS
212-248-0200
avsnyc@avs.org
www.avs.org



DIVISION/GROUP PROGRAMS:

- Advanced Surface Engineering
- Applied Surface Science
- Biomaterial Interfaces
- Electronic Materials & Processing
- Magnetic Interfaces & Nanostructures
- Manufacturing Science & Technology
- MEMS & NEMS
- Nanometer-Scale Science & Technology
- Plasma Science & Technology
- Surface Science
- Thin Film
- Vacuum Technology

FOCUS TOPICS:

- Actinides & Rare Earths
- Biofilms & Biofouling: Marine, Medical, Energy
- Biointerphases
- Electron Transport at the Nanoscale
- Energy Frontiers
- Exhibitor Technology Spotlight
- Graphene & Related Materials
- Helium Ion Microscopy
- InSitu Microscopy & Spectroscopy
- Nanomanufacturing
- Oxide Heterostructures-Interface Form & Function
- Scanning Probe Microscopy
- Spectroscopic Ellipsometry
- Transparent Conductors & Printable Electronics
- Tribology

Secondary electron deposition mechanism of carbon contamination

Adam F. G. Leontowich^{a)} and Adam P. Hitchcock

Brockhouse Institute for Materials Research, McMaster University, Hamilton, Ontario L8S 4M1, Canada

(Received 30 January 2012; accepted 13 March 2012; published 30 March 2012)

Deposition of a carbonaceous contaminant layer on surfaces exposed to radiation exceeding 7–10 eV is ubiquitous in many fields of research. The mechanism of this deposition process is still debated. A scanning transmission x-ray microscope has been used to create and interrogate carbonaceous deposits with photon energies spanning the C 1s ionization edge. For equal fluence, the rate of carbon deposition is proportional to the x-ray absorption spectrum of the deposited material. The results are consistent with a deposition mechanism involving secondary electrons. Implications of this measurement with regard to future generations of high volume photolithography are discussed. © 2012 American Vacuum Society. [<http://dx.doi.org/10.1116/1.3698602>]

I. INTRODUCTION

The step from the generally non-ionizing or only weakly ionizing light sources of 193 nm (6.4 eV) presently used in photolithographic tools for high volume integrated circuit production, to strongly ionizing light sources of 13.5 nm (92 eV) being introduced for extreme ultraviolet (EUV) lithography has the potential to introduce serious contamination issues due to radiation-induced cracking and deposition of carbonaceous molecules.^{1,2} The precursor molecules for such contamination originate from a wide variety of sources (lubricants, outgassing, atmosphere, etc.), and become fixed to surfaces as a carbonaceous layer when irradiated with ionizing radiation. This phenomenon is common to diverse technologies that involve high energy radiation (electron microscopy,^{3–5} x-ray photoelectron spectroscopy,⁶ synchrotron and free electron laser beamlines,^{7–9} space-based telescopes^{10–13}). The carbonaceous deposits are often highly undesirable as they can degrade the transmissive or reflective properties of optics, introduce spectroscopic artifacts, and/or decrease the efficiency of detectors. With regards to EUV lithography, the carbonaceous layer has been observed to decrease reflected intensity, distort the wavefront,¹⁴ and change the optical path length,⁹ all conceivably capable of introducing defects in the devices produced and reducing throughput. Several methods of cleaning carbonaceous deposits from delicate optics exist.^{2,5,8,11,12,15–17} The results are sometimes mixed,^{8,9,12} but in certain cases the reflectance can be fully recovered,¹⁵ and an optic can survive multiple cleaning cycles.¹⁷ In practice, the contamination processes can be mitigated,^{5,7,18} but often cannot be totally eliminated, and cleaning processes entail some instrument downtime, which ultimately reduces productivity. The precise mechanism of deposition is a matter of debate. A mechanism based on secondary electrons (SEs) produced by the irradiated surface is the most established.⁷ However,

Hollenshead and Klebanoff concluded that the dominant mechanism of deposition is direct photoabsorption by the adsorbed precursor molecules, and that the SE mechanism plays an insignificant role.¹⁹ In this Letter, the relationship between the rate of carbon deposition and photon energy is probed in the vicinity of the C 1s (*K*) ionization edge to illuminate the mechanism of deposition.

II. EXPERIMENT

Scanning transmission x-ray microscopes (STXMs)^{20,21} routinely focus monochromatic soft x-ray photons (60–2500 eV) into an intense, sub-30 nm full width half maximum spot at the focal plane. Carbon deposits tens of nanometers thick can be created on surfaces within seconds to minutes. The Advanced Light Source (ALS) STXM 5.3.2.2²⁰ at Lawrence Berkeley National Laboratories was used to create carbon deposits on an initially clean 75 nm thick Si₃N₄ surface. With a STXM, one can accurately control and rapidly vary the conditions of deposition, such as photon energy (with a bandwidth as low as 0.05 eV), area irradiated, fluence [photons/s (s⁻¹) × dwell time (s) × photon energy (J)/area (nm²)] and fluence rate. The STXM 5.3.2.2 chamber is a low vacuum environment, capable of only 10⁻⁶ Torr. For these experiments, the chamber was evacuated then backfilled with 250 Torr He. Areas of 600 nm × 600 nm consisting of 10 × 10 single pixel exposures were irradiated to form the deposits. The thickness of the deposited material was quantified by two techniques; measuring the maximum height of the deposit by atomic force microscopy [(AFM) ± 1 nm], and measuring the average optical density [(OD) ± 0.02] at 293 eV of the center of the deposit with the STXM. The precursor molecules for the deposits created here probably include those which originate partly within the STXM chamber (lubricants from mechanical stages, outgassing, or ablated organics from previous samples), and partly outside the chamber (fingerprints, venting the chamber to atmosphere, double-sided tape and epoxy used to mount samples).

^{a)}Electronic mail: leontoaf@mcmaster.ca

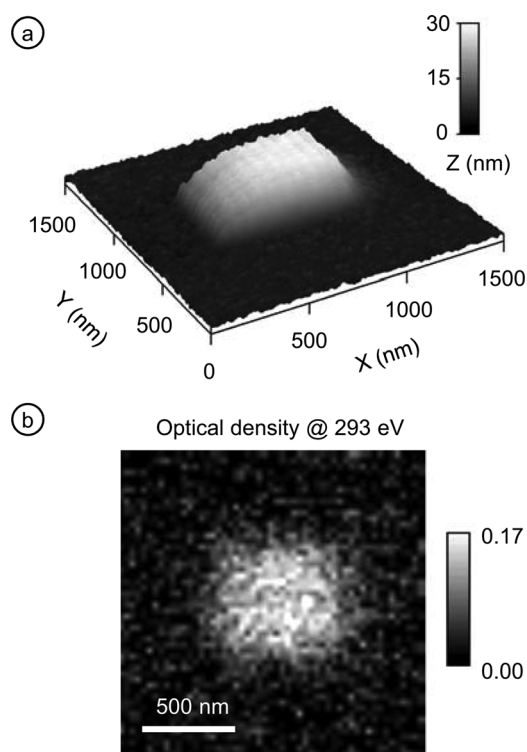


FIG. 1. Images of a $600 \text{ nm} \times 600 \text{ nm}$ carbon deposit created by focused 300 eV soft x rays of a scanning transmission x-ray microscope (STXM), recorded by (a) atomic force microscopy in tapping mode, and (b) STXM at 293 eV [transmission measurement converted to optical density (OD)].

III. RESULTS AND DISCUSSION

Several carbon deposits were made at the specific photon energy of 300 eV with increasing fluence. These deposits were imaged and quantified by AFM and STXM (Fig. 1). The rate of deposition observed was directly proportional to fluence (Fig. 2), which is consistent with the observations of others.^{7,15,18,19} The fluence involved in collecting single images for OD measurements was $0.5 \pm 0.1 \text{ mJ/cm}^2$.

A near edge x-ray absorption fine structure (NEXAFS) spectrum of the carbon deposit material in the $\text{C } 1s$ NEXAFS region (Fig. 3) was collected with the STXM in a second mode of operation where the sharp focus was maintained on

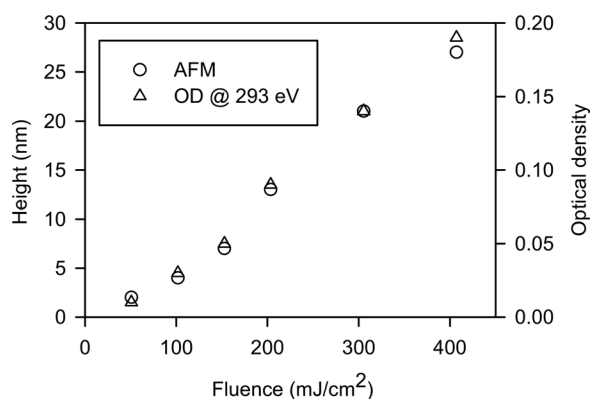


FIG. 2. Amount of carbonaceous material deposited at a single energy (300 eV) vs fluence, quantified by atomic force microscopy (circles) and STXM (OD at 293 eV , triangles).

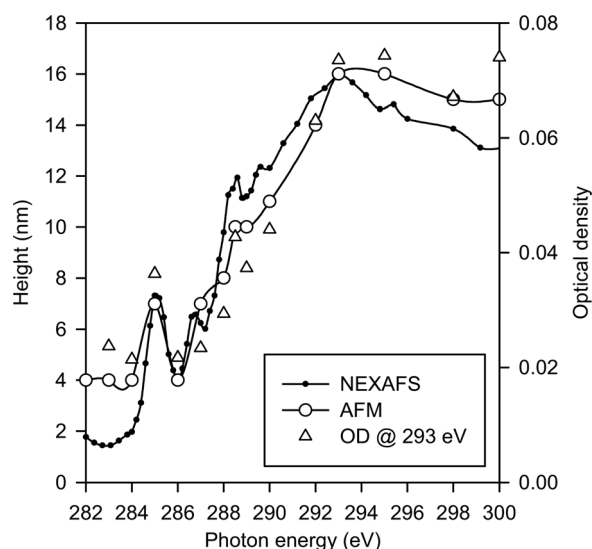


FIG. 3. $\text{C } 1s$ x-ray absorption (NEXAFS) spectrum of a carbon deposit (dots) compared to the amount of carbonaceous material deposited at constant fluence ($395 \pm 13 \text{ mJ/cm}^2$) at several specific photon energies, quantified by atomic force microscopy (circles) and STXM (OD at 293 eV , triangles).

the carbon deposit while the monochromator energy was scanned. The fluence involved in collecting this spectrum was $24 \pm 5 \text{ mJ/cm}^2$. The spectrum shows a sharp feature at 285 eV , indicative of $\text{C}=\text{C}$ bonds, a feature at 288.5 eV potentially indicative of $\text{C}=\text{O}$ bonds, and a broad absorption maximum near 293 eV . NEXAFS spectra of carbon deposits made by the same method using another STXM [Canadian Light Source (CLS) beamline 10ID-1] under the same conditions were identical. The spectra of the carbon deposits at both the ALS and CLS are similar to a reported $\text{C } 1s$ NEXAFS spectrum of carbon deposited in a system expressly designed to evaluate contamination rates and phenomena for EUV optics.²² It appears that beam-deposited carbonaceous material tends to have the same chemistry and thus a similar spectrum, independent of the precursor material.

Areas were then irradiated at specific photon energies spanning the $\text{C } 1s$ NEXAFS region, forming carbon deposits as a function of photon energy (Fig. 3). Each area irradiated received the same fluence of $395 \pm 13 \text{ mJ/cm}^2$. The fluence rate available at each energy differed between 74 and $388 \text{ mJ/cm}^2/\text{s}$ due to carbon contamination on the beamline and STXM optics; therefore the dwell times were varied to establish the desired fixed total fluence condition. In a separate experiment, the thickness of deposits made at specific photon energies at the same total fluence was observed to be independent of fluence rate over the same $74\text{--}388 \text{ mJ/cm}^2/\text{s}$ range. Figure 3 shows that, for constant fluence, the rate of carbon deposition is strikingly proportional to the $\text{C } 1s$ NEXAFS spectrum of the carbon deposit material. Most notably, the prominent spectral feature at 285 eV is reflected in the quantity of material deposited; the deposition rate at 285 eV is significantly greater than at 284 or 286 eV , in accord with the spectrum. The maximum deposition rate occurred at 293 eV , coinciding with the maximum absorption cross section of the carbon deposit material.

IV. SUMMARY AND CONCLUSIONS

The number of SEs emitted by a substance irradiated with x-rays is proportional to its x-ray absorption spectrum, which is the basis of the total electron yield (TEY) acquisition mode.²³ Note that this approximation is widely accepted to be valid over short photon energy ranges, such as that in Fig. 3, but careful examination over large energy spans indicates that it is necessary to take into account other factors, in particular photon energy variations in the number of primary electrons produced, in order to have a fully quantitative agreement.²⁴ The results are consistent with a deposition mechanism primarily involving SEs. The rate of carbon deposition follows the spectrum of the carbon deposit material because the deposition process is driven by SEs emitted by the surface, and the surface rapidly becomes deposited carbon once the deposition is initiated. For an equal fluence, the number of SEs emitted by the carbon deposit when irradiated at 285 eV is significantly higher than at 284 or 286 eV, which leads to the higher deposition rate at that particular photon energy. For deposits less than about 4 nm thick (less than the escape depth), the SE emission of the underlying surface (Si_3N_4 in this case) should play a greater role, which may be why the data points in the pre-edge region of Fig. 3 are higher than the NEXAFS spectrum. If the mechanism of deposition was primarily direct photoabsorption by the adsorbed precursor molecules, the rate of deposition should be closely linked to the C 1s NEXAFS spectra of saturated hydrocarbons^{23,25} which do not contain features at 285 eV and have very prominent absorption features between 287 and 289 eV. This is not what was observed.

This result suggests a possible contamination mitigation strategy: For a given photon energy, the irradiated surface with the lowest TEY should display the lowest deposition rate. Ru, widely used as a capping layer for 13.5 nm EUV optics, conveniently approaches a minimum electron yield value around 13.5 nm. This minimum in TEY has been hypothesized as a reason why Ru performs so well in this role.¹⁸ However, this mitigation strategy would only be effective until a carbon contamination layer of a few nanometers forms.

What are the implications of these results for high volume photolithography? The industry standard photon energy (wavelength) used for the critical layers has increased (decreased) stepwise over time,²⁶ which has been a major reason why the size of integrated circuits and the devices that employ them have steadily decreased while performance has increased. This “wavelength scaling” is expected by some to continue²⁷ beyond the expected to be state-of-the-industry of 13.5 nm; research and development is already under way on a second generation of sources and optics for sub-10 nm “beyond EUV” systems. Early candidate wavelengths include 6.7, 3.37, and 2.48 nm.²⁷ The first two of these wavelengths approach the C 1s ionization edge, while the third exceeds it. We have shown that for equal fluence, the rate of carbon deposition is roughly four times higher above the edge than below it. This work indicates that, if future high volume photolithography tools operate at a

wavelength at or above the C 1s edge, the rate of carbon deposition on the optics will increase substantially. Perhaps the increase in deposition rate might be offset by an increase in resist sensitivity, if C-based photoresists continue to be used, as the x-ray absorption cross section will increase above the C 1s edge for all C-based materials. The composition of the resists remains an open question, even for 13.5 nm. Early identification of challenges in wavelength scaling will narrow the choices, and ultimately decrease the time necessary to develop and implement new technology.

ACKNOWLEDGMENTS

This research was funded by NSERC, CFI, and the Canada Research Chairs program and carried out at ALS beamline 5.3.2.2 and CLS beamline 10ID-1. The authors thank David Kilcoyne and Tolek Tyliczszak for support at the ALS and Jian Wang, Yingshen Lu, and Chithra Karunakaran for support at the CLS. The ALS is supported by the Director, Office of Science, Office of Basic Energy Sciences, of the U.S. Department of Energy under Contract No. DE-AC02-05CH11231. The CLS is supported by NSERC, CIHR, NRC, and the University of Saskatchewan. A.F.G.L. acknowledges the support of an ALS doctoral fellowship in residence.

¹R. L. Stewart, *Phys. Rev.* **45**, 488 (1933).

²S. Bajt, in *EUV Lithography*, edited by V. Bakshi (SPIE, Bellingham, WA, 2009), pp. 227–259.

³J. Hillier, *J. Appl. Phys.* **19**, 226 (1948).

⁴P. Roediger, H. D. Wanzenboeck, G. Hochleitner, and E. Bertagnolli, *J. Vac. Sci. Technol. B* **27**, 2711 (2009).

⁵A. E. Vladár, K. P. Purushotham, and M. T. Postek, *Proc. SPIE* **6922**, 692217 (2008).

⁶D. R. Cousens, B. J. Wood, J. Q. Wang, and A. Atrons, *Surf. Interface Anal.* **29**, 23 (2000).

⁷K. Boller, R.-P. Haelbich, H. Hogrefe, W. Jark, and C. Kunz, *Nucl. Instrum. Methods Phys. Res.* **208**, 273 (1983).

⁸R. A. Rosenberg, J. A. Smith, and D. J. Wallace, *Rev. Sci. Instrum.* **63**, 1486 (1992).

⁹S. Bajt *et al.*, *Proc. SPIE* **7361**, 73610J (2009).

¹⁰E. M. Wooldridge, NASA Technical Report No. 19980237489 (1998).

¹¹J. L. Tveekrem, D. B. Leviton, C. M. Fleetwood, and L. D. Feinberg, *Proc. SPIE* **2864**, 246 (1996).

¹²R. B. Gillette and B. A. Kenyon, *Appl. Opt.* **10**, 545 (1971).

¹³H. L. Marshall, A. Tennant, C. E. Grant, A. P. Hitchcock, S. L. O'Dell, and P. P. Plucinsky, *Proc. SPIE* **5165**, 497 (2004).

¹⁴A. Barty and K. A. Goldberg, *Proc. SPIE* **5037**, 450 (2003).

¹⁵K. Hamamoto *et al.*, *J. Vac. Sci. Technol. B* **23**, 247 (2005).

¹⁶R. W. C. Hansen, M. Bissen, D. Wallace, J. Wolske, and T. Miller, *Appl. Opt.* **32**, 4114 (1993).

¹⁷S. A. George, L. M. Baclea-an, P. P. Naulleau, R. J. Chen, and T. Liang, *J. Vac. Sci. Technol. B* **28**, C6E31 (2010).

¹⁸B. V. Yakshinsky, R. Wasielewski, E. Loginova, and T. E. Madey, *Proc. SPIE* **6517**, 65172Z (2007).

¹⁹J. Hollenshead and L. Klebanoff, *J. Vac. Sci. Technol. B* **24**, 64 (2006).

²⁰A. L. D. Kilcoyne *et al.*, *J. Synchrotron Radiat.* **10**, 125 (2003).

²¹M. Howells, C. Jacobsen, and T. Warwick, in *Science of Microscopy*, edited by P. W. Hawkes and J. C. H. Spence (Springer, Berlin, 2006), pp. 835–926.

²²M. Niibe *et al.*, *J. Vac. Sci. Technol. B* **25**, 2118 (2007).

²³J. Stöhr, *NEXAFS Spectroscopy* (Springer, Berlin, 1992).

²⁴H. Henneken, F. Scholze, and G. Ulm, *J. Appl. Phys.* **87**, 257 (2000).

²⁵A. Schöll, R. Fink, E. Umbach, G. E. Mitchell, S. G. Urquhart, and H. Ade, *Chem. Phys. Lett.* **370**, 834 (2003).

²⁶C. Wagner and N. Harned, *Nature Photon.* **4**, 24 (2010).

²⁷G. Tallents, E. Wagenaars, and G. Pert, *Nature Photon.* **4**, 809 (2010).